Oxidized Ultrashort Nanotubes as Carbon Scaffolds for the Construction of Cell-Penetrating NF-κB Decoy Molecules

Rita Crinelli,[†,*] Elisa Carloni,[†] Michele Menotta,[†] Elisa Giacomini,[†] Marzia Bianchi,[†] Gianluca Ambrosi,[‡] Luca Giorgi,[‡] and Mauro Magnani[†]

[†]Department of Biomolecular Sciences, Biochemistry and Molecular Biology Section and [‡]Institute of Chemical Sciences, University of Urbino "Carlo Bo", 61029 Urbino (PU), Italy

ABSTRACT Oligonucleotide (ODN) decoys are synthetic ODNs containing the DNA binding sequence of a transcription factor. When delivered to cells, these molecules can compete with endogenous sequences for binding the transcription factor, thus inhibiting its ability to activate the expression of target genes. Modulation of gene expression by decoy ODNs against nuclear factor-κB (NF-κB), a transcription factor regulating many genes involved in immunity, has been achieved in a variety of immune/inflammatory disorders. However, the successful use of transcription factor decoys depends on an efficient means to bring the synthetic DNA to target cells. It is known that single-walled carbon nanotubes (SWCNTs), under certain conditions, are able to cross the cell membrane. Thus, we have evaluated the possibility to functionalize SWCNTs with decoy ODNs against NF-κB in order to improve their intracellular delivery. To couple ODNs to CNTs, we have exploited the carbodiimide chemistry which allows covalent binding of amino-modified ODNs to carboxyl groups introduced onto SWCNTs through oxidation. The effective binding of ODNs to nanotubes has been demonstrated by a combination of microscopic, spectroscopic, and electrophoretic techniques. The uptake and subcellular distribution of ODN decoys bound to SWCNTs was analyzed by fluorescence microscopy. ODNs were internalized into macrophages and accumulated in the cytosol. Moreover, no cytotoxicity associated with SWCNT administration was observed. Finally, NF-κB-dependent gene expression was significantly reduced in cells receiving nanomolar concentrations of SWCNT—NF-κB decoys compared to cells receiving SWCNTs or SWCNTs functionalized with a nonspecific ODN sequence, demonstrating both efficacy and specificity of the approach.

KEYWORDS: carbon nanotubes · ODN decoy · NF-κB · macrophages · inflammation · drug delivery · regulation of gene expression

Oligonucleotides (ODNs) are potential therapeutic agents with several attractive properties, including selective recognition of molecular targets, which results in high specificity of action.[1] ODNs can operate *via* different mechanisms to control gene expression at either the transcriptional or the post-transcriptional level. Synthetic double-stranded ODNs (dsODNs), containing the consensus binding sequence of a transcription factor, compete for binding of transcription factors with their consensus sequence in target genes.[2] Thus, once delivered into cells, the ODN acts as a trap for the target factor, allowing selective modulation of gene expression. The decoy technology has proven effective both *in vitro* and *in vivo*, suggesting its use in therapy.[3] Several decoy molecules are already or will be briefly under clinical trial.[4,5] On the other hand, the number of diseases which could be potentially treated with ODN decoy therapeutics is increasing with the growing of transcription factors found to be involved in human disease pathogenesis.

The nuclear factor-κB (NF-κB) plays a critical role in regulating expression of genes responsible for a wide range of cellular processes, including innate and adaptive immune responses and pathways related to cell survival and proliferation. Therefore, it is considered a good target for therapeutic interventions, primarily in situations of chronic inflammation or in cancer, where the NF-κB pathway is often constitutively active and plays a key role in the disease.[6] The proof of concept that NF-κB ODN decoys can function as drugs for the treatment of a variety of disorders has been provided by several groups in a set of different chronic inflammatory and autoimmune disease models such as cardiovascular diseases and ischemia reperfusion injury, intimal hyperplasia, asthma, rheumatoid arthritis, and atopic dermatitis.[7] However, the successful use of transcription factor decoys, as for other ODN strategies, almost always depends on an efficient means to bring the synthetic DNA to target tissues, cells, and, eventually, cellular compartments.[1] Indeed, cellular uptake of naked DNA is an extremely inefficient process due

*Address correspondence to rita.crinelli@uniurb.it.

Received for review January 11, 2010 and accepted April 18, 2010.

Published online April 22, 2010. 10.1021/nn100057c

Figure 1. Schematic representation of the NF-κB decoy molecule. The NF-κB decoy consisted of a 30-mer double-stranded oligonucleotide containing two copies of the κB site (in bold, underlined), present in the PRDII domain of the human IFN-β promoter, capped with unrelated extra sequences of 5 nt at both terminal ends. The sense strand was amino-modified in order to covalently couple the ODN to oxidized CNTs. C6 indicates the 6 atom carbon linker connecting the amino group to the 5′ end.

to the existence of natural barriers which obviously counteract the intracellular transfer of exogenous DNA. Thus, the transition of DNA-based therapeutics, including decoys, into drugs is critically dependent on the development of DNA delivery platforms designed to avoid the biological barriers to DNA uptake. Several vectors to improve ODN decoy intracellular delivery have been described and are currently developed, including positively charged lipids, liposomes, and cell-penetrating peptides.[8,9] Cationic liposomes are largely used to facilitate ODN uptake into cells both *in vitro* and *in vivo*.[8,10] However, the efficiency of these vectors is still low, making it necessary to use large amounts of these lipids to achieve acceptable levels of transfection, with consequent toxic side effects. Therefore, to be translated into the clinic, more efficient liposome formulations need to be designed in order to reduce the dose necessary to achieve therapeutic efficacy.[11] An alternative and interesting approach is that based on the combination of the hemagglutinating virus of Japan (HVJ) and liposomes. This method is a liposome-based gene transfer strategy that enables delivery of the contents of liposomes directly into the living cells by means of the virus−cell fusion machinery. It has been successfully employed to mediate ODN decoy delivery *in vivo*,[12] although concerns about the safety of using viral systems in humans could limit its therapeutic application. Successful delivery of ODN decoys was also obtained using mechanical transfection methods.[13] However, this is not an approach that can be easily adapted to a clinical setting, being useful only for *ex vivo* or *in situ* applications. Thus, novel materials that will facilitate effective delivery of ODN decoys are also being explored and may offer an alternative to and/or improve the currently available systems. In this respect, carbon nanotubes (CNTs) seem to represent ideal candidates as potential vectors for delivering ODN decoys. The rationale relies on the observation that several functionalization schemes that allow coupling of biological molecules to carbon nanotubes have been developed. In addition, and most importantly, it has been demonstrated that CNTs have the ability to penetrate mammalian cells and transport various cargos inside cells, including peptides, proteins, and nucleic acids.[14] The cell penetration mechanism and the intracellular dynamic fate of the internalized CNTs are still a matter of debate. In this context, also interesting, is the observation that SWCNTs (single-walled CNTs) seem to prolong the circulation time as well as the bioavailability of conjugated molecules.[15] Thus, the possibility that CNTs can be used as innovative carriers for drug delivery represents at the moment an area of intensive investigation. Concerning nucleic-acid-based therapeutics, several reports have demonstrated that SWCNTs represent an effective delivery system for application in siRNA-mediated gene silencing.[16−18] Similarly, Cui *et al.* have provided demonstration that antisense-modified SWCNTs can be used for intracellular gene regulation.[19] Up to now, however, to the best of our knowledge, no studies have addressed the possible use of SWCNTs for delivering transcription factor decoy molecules.

In this work, we have used the carbodiimide chemistry to cross-link ODN decoys against NF-κB to SWCNTs. Using a combination of techniques, such as AFM (atomic force microscopy), ESI-MS (electrospray ionization mass spectrometry), and EMSA (electrophoretic mobility shift assay), the adducts have been characterized from a physical, chemical, and biological point of view, respectively, providing evidence that our approach was indeed effective in producing conjugates, where partners interact in a covalent manner, without losing the ability to function as transcription factor decoys. The uptake, intracellular distribution, and efficacy of decoy ODNs, once bound to SWCNTs, were then studied using monocyte-derived human macrophages as a model. Indeed, macrophages represent one of the most important cellular compartments involved in immune/inflammatory reactions, and NF-κB has been shown to regulate various pathways that impact the function of these cells. Results presented provide the very first evidence that SWCNTs are capable of efficiently delivering decoy molecules, obtaining sequence-specific down-regulation of NF-κB-dependent gene expression with nanomolar concentrations of dsODN. This work expands to decoy ODNs the list of bioactive molecules which can be delivered using CNTs as vectors.

RESULTS AND DISCUSSION

Decoy Design. Oligonucleotide decoys for NF-κB have been described previously[20] and are schematically represented in Figure 1. In the context of the present work, the criterion for introducing two κB sites was based on the observation that ODN decoys containing multiple identical *cis* elements have remarkably greater efficacy and potency of action than ODNs containing only one *cis* element, thus allowing reduction of molar concentration and, as a consequence, toxicity.[10] Furthermore, 5 nt long extra sequences were inserted at both terminal ends and on both strands in order to provide an extra spacer arm in addition to the C6 linker and to better support NF-κB binding. Indeed, crystallographic studies have highlighted that NF-κB establishes DNA backbone contacts also outside the 10 bp κB site.[21]

Coupling of ODN Decoys to SWCNTs and Characterization of the Adducts. It has been reported that single-stranded DNA can interact very strongly with SWCNTs in water through nucleic acid−base stacking on the nanotube surface.[22,23] By contrast, adsorption of double-stranded DNA seems to be a very less favorable process due to the hydrophilic nature of the external surface of DNA.[24] On the other hand, because of the negative charges on the phosphate groups along the DNA backbone, positively charged SWCNTs have been employed to mediate gene delivery and expression leading to the production of proteins encoded in double-stranded plasmid DNA.[25] Compared to noncovalent interactions, covalent bonding is expected to allow control of the location of the biomolecule and to improve stability and accessibility, which are important features for a biomolecule that must function as a "decoy". Thus, for the immobilization of the NF-κB ODN decoy onto SWCNTs, we have exploited a process of diimide-activated amidation between carboxylic acid groups on acid-oxidized SWCNTs (SWCNT-O) and amino groups positioned at the 5′ end of double-stranded ODNs. In contrast to the CNT−dsODN conjugates obtained by Hazani *et al.*[26] and Zhang *et al.*,[18] consisting of CNTs functionalized with single-stranded ODNs, which were later annealed with the complementary strand, our approach involved direct binding of the double-stranded species. We reasoned that this strategy should indeed minimize DNA adsorption which, as explained above, is strongly associated with single-stranded rather than double-stranded DNA molecules. Indeed, since adsorption may be dominating over slower covalent reactions, once occurred, adsorbed molecules may shield adjacent carboxylic groups from reacting with other molecules.[27] Activation efficiency of nanotube-associated carboxylic acid groups was evaluated by assaying SWCNT-O concentration in the supernatant obtained after activation, ultrafiltration, and centrifugation of the retentate. Indeed, while in the absence of acylating agents the majority of SWCNT-O present in the retentate precipitated following centrifugation (Figure 2A), activated SWCNT-O remained soluble (Figure 2B). Thus, the amount of SWCNTs present in the supernatant, as determined spectrophotometrically at 808 nm, can provide an indirect measure of the activation efficiency. In order to set up the reaction, different EDAC (*N*-(3-dimethylaminopropyl)-*N*′-ethyl carbodiimide hydrochloride) concentrations, corresponding to 10, 40, 160, and 320 mM, were tested in reactions where the amount of NHSS (*N*-hydroxysulfosuccinimide sodium salt) was maintained fixed at 35 mM (Figure 2B,C). Efficient activation was already observed with a carbodiimide concentration of 40 mM (Figure 2C). Indeed, lower amounts were less effective, and by contrast, higher amounts did not significantly further increase CNT solubility. The effects of NHSS amount were subsequently evaluated by keeping EDAC fixed at 40 mM and using

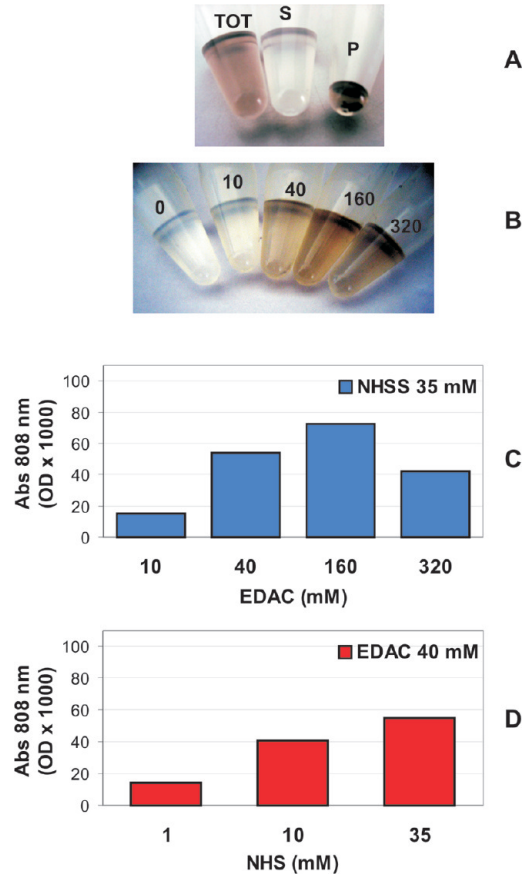

Figure 2. Effect of EDAC and NHSS concentration on the activation efficiency of nanotube-associated COOH groups. (A) In the absence of acylating agents, SWCNT-O precipitated after centrifugation (TOT, before centrifugation; S, supernatant, and P, pellet, after centrifugation). (B) By contrast, when activated using different EDAC concentrations (from 10 to 320 mM), SWCNT-O remained soluble and could be recovered in the supernatant. Thus, the amount of soluble SWCNT-O in the supernatant, as spectrophotometrically measured at 808 nm, was used to determine the activation efficiency with different concentrations of EDAC, in the presence of a fixed amount of NHSS (C) and with different concentrations of NHSS, using a fixed amount of EDAC (D).

1, 10, or 35 mM NHSS (Figure 2D). From these experiments, it has been established that a significant improvement in the activation efficiency was obtained with 10 mM NHSS compared to 1 mM, while 35 mM NHSS did not further improve the reaction performance (Figure 2D). Thus, 40 mM EDAC and 10 mM NHSS were chosen to run subsequent coupling reactions. EDAC/NHSS activation of carboxyl groups is typically carried out under buffered acidic conditions which allow prolonged half-life of the NHSS ester. On the other hand, the EDAC−NHSS coupling reaction occurs *via* the free amines and not the protonated ones. In acidic pH, terminal alkyl amines of the amino-modified ODNs are mostly protonated, hence, acidic pH does not favor the coupling reaction. In order to overcome these problems, the activation reaction was performed at pH 5.5, while for the coupling step, the pH was raised to 8.0, a value which is usually optimal for ODN conjugation.

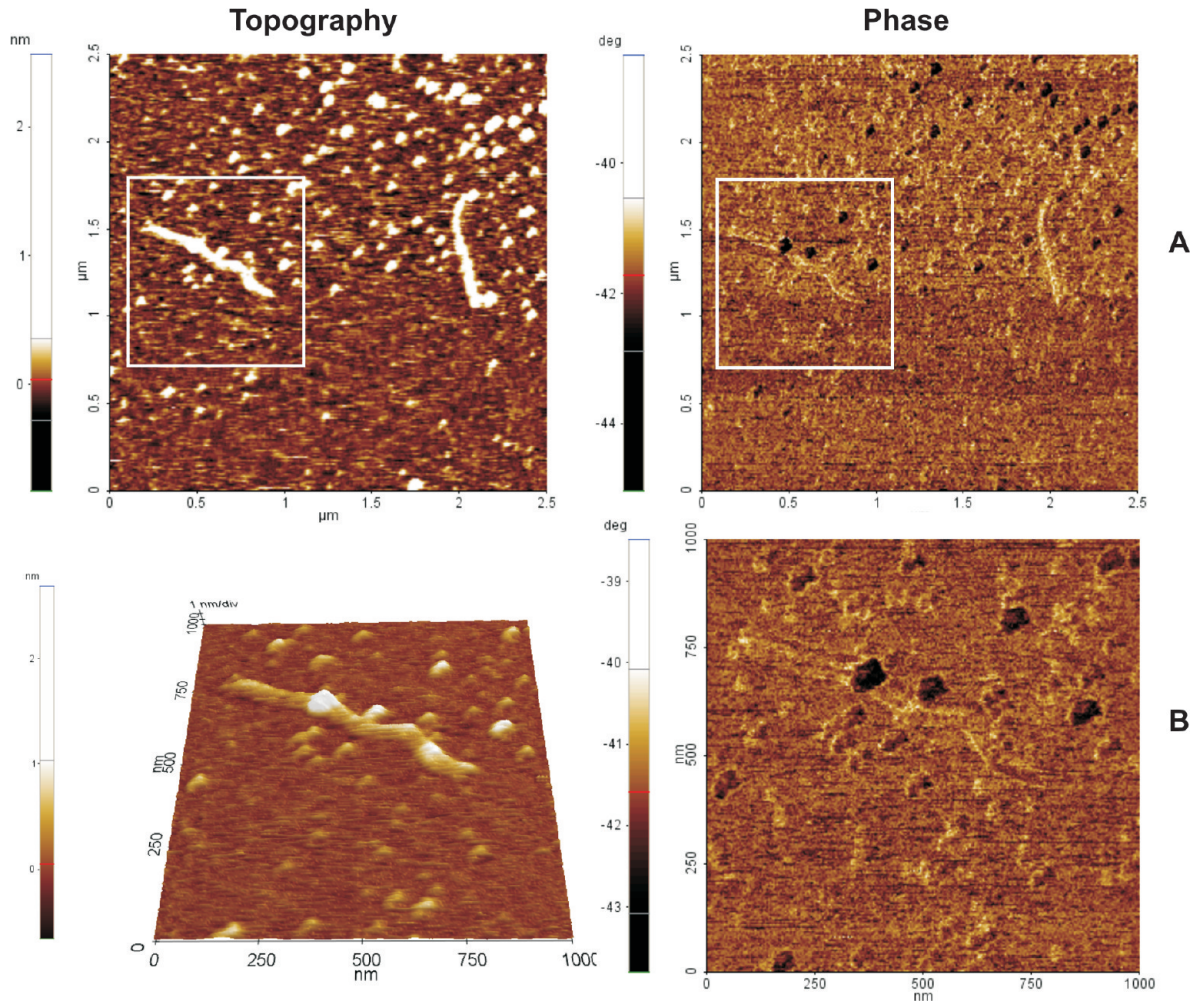

Figure 3. (A) AFM images of SWCNT-O functionalized with the NF-κB ODN decoy revealing that most of the oxidized SWCNTs consisted of ultrashort nanotube fragments with few exceptions (left panel). ODNs appear in phase imaging as darker regions (right panel). (B) Zoomed scan corresponding to the boxed area in panel A.

AFM topography showed that SWCNT-O mostly consisted of ultrashort nanotube fragments with heights consistent with those of individual nanotubes (<1.5 nm) and lengths less than 100 nm (Figure 3A). SWCNT-O with lengths lower that 50−100 nm have also been obtained by other groups which have demonstrated that the oxidative cutting of SWCNTs can cause them to be drastically shortened.[28,29] AFM phase imaging was used to obtain a visual confirmation of the ODN attached to SWCNT-O. Indeed, the phase imaging signal provides information on differences in surface chemical properties, thus allowing one to distinguish DNA molecules from the SWCNT surface.[30] This type of analysis confirmed that at least some ODN molecules were bound to CNTs, as demonstrated by an increase in phase lag (shown as a darker region) in coincidence of certain SWCNT-O identified in the topography region. In particular, for the shorter fragments, it has been impossible to physically discriminate the nanotube surface from the ODN structure, with the two interacting moieties' molecular dimensions similar and, presumably, under the lateral resolution capacity of AFM (Figure 3A). Although uncoupled oligonucleotides were removed from the reaction mixture by extensive ultrafiltration of the preparation, at this stage, we could not exclude that darker spots in the phase image might be due to the presence of residual free ODNs. On the other hand, supposing that these phase signals correspond to free ODNs, we should imagine that most of the ODNs were uncoupled, which is in contrast with further analyses (see below). The association between ODNs and SWCNTs was evident in some of the longer fragments, where the functional groups appear appended to discrete areas along the CNT axis (Figure 3B). This localization is consistent with the notion that carboxylic acid groups, which are introduced by oxidation with strong acids, occur at the open end and/or at defect sites along tube walls.[14] Thus, the evidence that the distribution of ODNs onto CNTs involves distinct areas, rather than the whole surface, suggests that oligonucleotides are specifically bound to nanotubes and not physically adsorbed to CNT walls.

To further characterize SWCNT−ODN adducts, they were submitted to ESI-MS analysis. As control, EDAC/

NHSS-activated SWCNT-O and SWCNT-O incubated with the ODN in the absence of EDAC/NHSS, were used. As depicted in Figure 4A, the spectrum of oxidized nanotubes showed an almost continuous background of ion signals across the whole mass range with some more prominent signals over the background. Similar results have been obtained by Avdoshenko *et al.*[31] This kind of spectrum is consistent with a sample having a broad distribution of species in terms of both mass and charge (multiple charged species of close masses), as it is expected to obtain upon SWCNT oxidation. In contrast to SWCNT-O, nanotubes functionalized with the ODN had sharply different mass-to-charge (*m/z*) peak profile (Figure 4B), which did not resemble the spectrum of SWCNT-O incubated with the ODN in the absence of EDAC/NHSS (Figure 4C). This result is consistent with a scenario where most of the ODNs were bound to CNTs, reinforcing the hypothesis that the increase in the phase lag, observed in AFM, could be indeed attributed to CNT−ODN complexes rather than to free ODNs. Moreover, the evidence that nanotubes displayed markedly different peak distribution and intensity only when carboxylated SWCNTs were incubated with the acylating agents before adding the ODN (Figure 4, compare panels B and C with A) supports the conclusion that the oligonucleotide is indeed covalently bound to CNTs and not simply adsorbed.

Since ODN decoy end-attachment should favorably present the ligand on the surface of the CNT such that the bound ODN can retain the ability to interact with the target factor, quantification of the amount of ODN immobilized on SWCNT-O was indirectly assessed by competitive EMSA, which also allows testing of the functionality of the bound molecule as a decoy. Indeed, as described in Methods, this assay exploits the ability of the SWCNT−ODN complex to compete with the free ^{32}P-labeled ODN for binding to NF-κB. While no competition was observed with samples derived from reactions performed with fluorescinated SWCNT (SWCNT-AAF), used as control, CNT−ODN conjugates were able to compete with the free ^{32}P-labeled probe for binding NF-κB (Figure 5).

Competition experiments and dose−response curves allowed us to establish that under this experimental condition a mean binding efficiency of 7.86 ± 1.2 (SD) pmol ODN/μg SWCNT-O is obtained ($n = 5$) (Figure 5).

Delivery of SWCNT−ODN Decoy Conjugates to Primary Human Macrophages. Monocyte-derived human macrophages were selected as target cells since macrophages are central to the body's immune/inflammatory responses. Similar to tissue macrophages, they are terminally differentiated and do not proliferate and are more relevant as a macrophage model than immortalized macrophage cell lines. To visualize SWCNT−ODN internalization by fluorescence microscopy, the antisense strand was purchased fluorescently labeled with FAM (6-carboxyfluorescein). SWCNTs conjugated to the same fluorophore (*i.e.*, fluorescein) were obtained by reacting EDAC/NHSS-activated carboxyl groups of SWCNT-O with the primary amine of 5-(aminoacetamido)fluorescein (fluoresceinyl glycine amide), a fluorescein derivative abbreviated as AAF. Fluorescinated SWCNTs (SWCNT−AAF) and the ODN−FAM alone were used as controls. As expected, free ODNs did not cross the cell membrane. Indeed, no green staining was observed after overnight incubation of the cells with the ODN−FAM added directly to the culture medium at a final concentration of 1 μM (Figure 6A). By contrast, SWCNT−AAF readily entered the intracellular milieu and accumulated in the cytosolic compartment (Figure 6A). This is demonstrated by the green fluorescent signal of CNT−AAF, which did not preferentially localize along the cell membrane, as it would occur if SWCNTs only stacked on the extracellular side, but showed a diffuse distribution within cells (Figure 6B). In addition, from the merge picture of panel B, it is evident that the green fluorescein signal was clearly distinct from DAPI-stained nuclei. Thus, at least in the limit of resolution of fluorescence microscopy that does not allow detection of individual nanotubes, most of the CNTs appear excluded from the nuclear area (Figure 6B). CNTs carrying the ODN decoy (SWCNT−ODN−FAM) were seen to enter the cells, as well, displaying the same intracellular distribution as SWCNT−AAF (Figure 6C). Again, the green fluorescent decoy ODN was observed intracellularly but, in most of the cases, was distinct from nuclear DNA staining, as it can be appreciated from overlaid images (Figure 6C,D). A picture taken at a lower magnification demonstrates that the vast majority of the cells were transfected with the FAM-labeled ODN (Figure 6D). It is known that short oligonucleotides delivered to the cell cytosol can readily internalize into the cell nucleus.[32] In contrast, for ODN decoys conjugated to SWCNTs, we observed cellular internalization but apparently not nuclear translocation, as reported also by other groups with other nucleic-acid-based molecules covalently bound to CNTs.[17] These observations suggest that, without the release of DNA from SWCNT transporters, the ODN is unable to penetrate the nuclear membrane.

Efficacy of Delivered SWCNT−ODN Decoy Conjugates in Suppressing NF-κB-Dependent Gene Expression upon LPS Stimulation. While most transcription factors are activated into the nucleus, NF-κB activation requires nuclear translocation. Therefore, if ODN decoys covalently linked to CNTs are retained in the cytosol, their cellular localization should not affect their efficacy.

Monocyte-derived human macrophages were incubated overnight with ODN decoys against NF-κB covalently coupled to SWCNTs (SWCNT−NF-κB decoy) at a final concentration of 11.3 ± 2.4 nM, corresponding to 1.72 ± 0.3 μg/mL SWCNTs, in the presence of lipopolysaccharide (LPS), which is known to induce

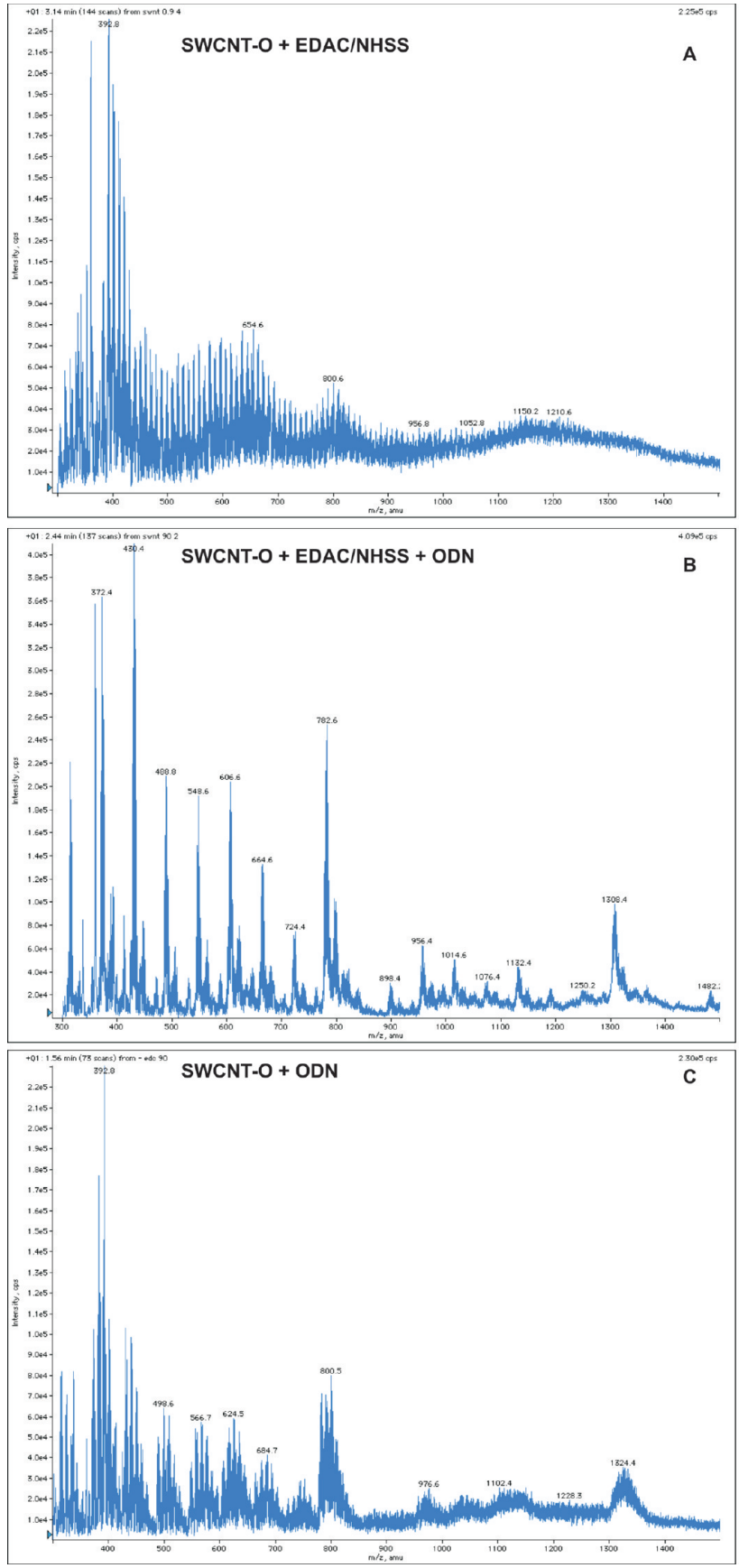

Figure 4. Positive ion mass spectra of EDAC/NHSS-activated SWCNT-O submitted to the coupling procedure in the absence (A) and in the presence of the ODN decoy (B). As control, EDAC/NHSS was omitted from the reaction and SWCNT-O was incubated with the ODN (C).

NF-κB activation in macrophages. As control, LPS-stimulated cells were treated with an equal amount of SWCNT−AAF (set as 100% NF-κB activation) or SWCNT carrying a scrambled ODN (SWCNT-SCRAMBLED decoy). SWCNT−AAF were selected as the control in order to have SWCNTs submitted to the same functionalization procedure of SWCNT−ODN. The scrambled sequence construct provided an additional control in order to exclude any nonspecific effect. Real-time PCR analysis of some selected NF-κB target genes revealed that mRNA levels of COX-2 (cyclooxygenase 2), IL-8 (interleukin 8), and IL-23 (interleukin 23) were 70, 50, and 60% reduced, respectively, upon cell treatment with SWCNT−NF-κB decoys with respect to cells receiving SWCNT−AAF conjugates (Figure 7). Interestingly, the products of these genes have been implicated in mediating a variety of autoimmune and inflammatory diseases.[33−35] No inhibition or a modest decrease (20%) in the expression of the same genes was observed in cells treated in parallel with SWCNT-SCRAMBLED decoys (Figure 7), thus demonstrating that the NF-κB decoy effect was indeed sequence-specific.

Compared to COX-2, IL-8, and IL-23, the IκBα (inhibitor kB) mRNA levels were markedly less affected, as demonstrated by only a 35% reduction detected after NF-κB decoy administration *versus* SWCNT−AAF-treated cells and considering a 20% inhibition measured in macrophages receiving the SCRAMBLED decoy (Figure 7).

Under our experimental conditions, it is expected that LPS triggers NF-κB activation before SWCNTs carrying the decoy molecules enter the cells. Indeed, NF-κB appears in the nucleus as soon as 15−30 min after LPS challenge (data not shown). However, no signal was observed upon 2 h incubation of the cells with SWCNT−AAF (data not shown), suggesting that SWCNT entrance is a process which occurs later than NF-κB activation. Moreover, it is known that NF-κB does not regulate all of its downstream genes in the same way. Some genes, such as IκBα, are early genes that are activated quickly by NF-κB; others are late genes that are activated only after prolonged exposure to NF-κB.[36] This could explain why IκBα, as an immediate accessible gene, does not appear affected by the decoy molecule activity, contrary to the other target genes analyzed. On the other hand, upon activation of the NF-κB signaling pathway, newly synthesized free IκBα binds to nuclear NF-κB, leading to export of the complex in the cytoplasm. In the presence of continuous stimulation, oscillations in NF-κB nuclear cytoplasmic localization that decrease in frequency during time have been described.[37] Thus, it could be speculated that the decoy, which remains in the cytosolic compartment, exerts its effect when NF-κB is transported back to the cytoplasm by trapping the transcription factor in this cellular compartment and avoiding its new nuclear translocation. On the whole, this would lead to a more quick dampening of the oscillations, thus mainly affecting expression of late genes, which depends on oscillation persistence.[37]

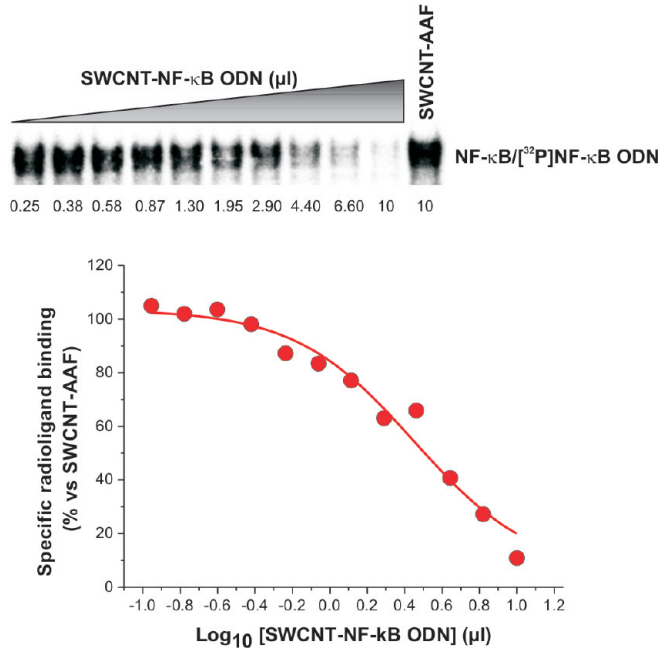

Figure 5. Quantification of the ODN bound to SWCNTs by competitive EMSA. Competition experiments were performed by incubating nuclear extracts from TNF-α-stimulated HeLa cells together with a fixed amount of the [^{32}P]-NF-kB ODN and increasing volumes (from 0.25 to 10 μL) of the different SWCNT−NF-κB ODN preparations (a typical experiment is shown). NF-kB/[^{32}P]−NF-κB ODN complex formation was analyzed by EMSA and quantified in a Molecular Imager. Data were expressed as percent binding relative to the signal detected when 10 μL of SWCNT-AAF, used as control, was added to the binding reaction. IC_{50} values were estimated by plotting these data as a function of the log10 of the competitor volume (μL) and fitting to a dose−response curve.

Cytotoxicity. The biocompatibility of foreign matter in living cells is an important point of concern. SWCNTs have been shown to be toxic in a number of cell types. Although toxicological data concerning SWCNTs are still fragmentary, it has become evident that CNT toxicity may be linked to several parameters, including catalyst contamination, dose, size, coating or surface functionalization, and aggregation status.[38] Raw SWCNTs with significant metal contamination have been shown to cause potentially adverse cellular responses in mesothelial cells through activation of signaling pathways associated with oxidative stress.[39] Commercial purified SWCNTs were seen to enter the cytoplasm forming bundles and localize also within the nucleus, causing cell mortality in a dose-dependent manner.[40] On the other hand, intraperitoneal injection of SWCNTs in mice has clearly demonstrated that tubes, irrespective of their length or dose, can coalesce inside the body to form fiber-like structures with consequent cytotoxicity. Indeed, high doses of even ultrashort tubes induced a granulomatosis reaction because of their ability to form aggregates.[41] In light of these findings, surface functionalization, which influences solubilization and the forma-

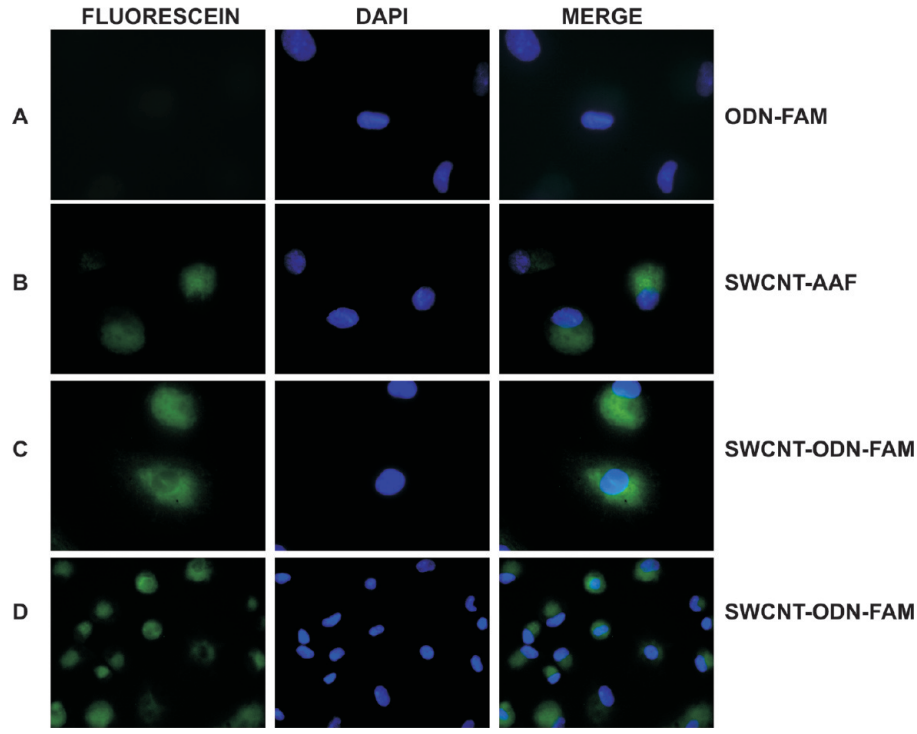

Figure 6. Representative fluorescence microscopy photographs of human monocyte-derived macrophages incubated overnight with (A) the ODN−FAM alone (final concentration in culture medium 1 μM), (B) SWCNT−AAF (final concentration in culture medium 1.8 μg/mL), or (C,D) SWCNTs functionalized with the ODN−FAM (SWCNT−ODN−FAM, final concentration in culture medium 1.8 μg/mL SWCNTs, corresponding to 14 nM CNT-bound ODN). The green fluorescence signal corresponds to fluorescein-labeled ODNs (A,C,D) and SWCNTs (B). Cell nuclei were visualized by DAPI staining of DNA (blue). In the last right column, images acquired with the appropriate filters have been merged. Pictures in panels A−C were taken with a magnification ×100 lens; picture in D with a 20× lens.

tion of stable suspensions, could have a strong impact on the biocompatibility of CNTs.

Concerning acid-oxidized SWCNTs, contradictory results have been reported. A recent paper by Porter *et al.* has demonstrated that acid-treated SWCNTs cause no significant changes in cell viability to monocyte-derived human macrophages, in sharp contrast to untreated SWCNTs.[42] In this paper, the authors conclude that the degree of cytotoxicity of CNTs seems dependent on various factors including the presence of metal catalyst particles, which are removed by acid treatment to generate oxidized CNTs, poor CNT solubility in water, which can be increased with chemical functionalization, and dimensions, which are reduced in acid-treated SWCNTs because of the fragmentation obtained in strong acidic conditions. In agreement with these observations, we found no significant differences in cell viability, as assessed by MTS assay, between untreated cells and cells incubated overnight with SWCNT−AAF or SWCNT−NF-κB decoy (Figure 8A). Furthermore, cells remained vital after 5 days from the exposure to SWCNTs. In contrast to the these observations, Saxena *et al.* have demonstrated that acid-functionalized SWCNT preparations exert toxic effects, and these effects can be reversed by neutralizing their surface charge with poly-L-lysine.[43] In our case, the covalent binding of functional groups (either fluorescein or the ODN) to carboxyl functions onto the CNT surface could have produced the same neutralizing effect of poly-L-lysine, thus explaining the absence of toxicity. In support of this hypothesis, oxidized carbon nanotubes complexed with proteins have been delivered to various mammalian cells without observing cytotoxicity.[44] Moreover, under our experimental conditions, no cleavage of caspase-3 was revealed by western immunoblot

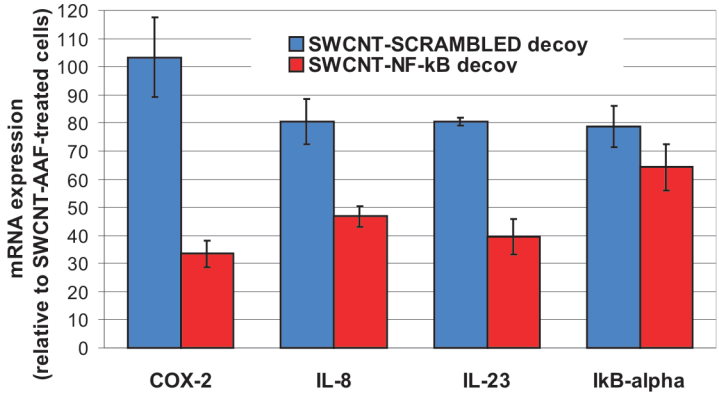

Figure 7. Real-time quantitative PCR analysis of NF-κB target gene expression upon delivery of SWCNT−NF-κB decoys. Total RNA, extracted from human macrophages incubated overnight with SWCNT−AAF, SWCNT−NF-κB decoy, or SWCNT-SCRAMBLED decoy in the presence of LPS, was amplified with primers specific for COX-2, IL-8, IL-23, and IkB-α genes. Expression data, normalized to the housekeeping B2M gene, were analyzed by the $2^{-\Delta\Delta CT}$ method, and the values were referred to the SWCNT−AAF-treated sample. Values are mean ± SEM of at least three independent experiments.

analysis of cellular extracts using a monoclonal antibody which detects endogenous levels of full-length (35 kDa) and large fragment (17/19 kDa) of caspase-3 (Figure 8B). Caspase-3 (cystenil aspartate-specific protease) is one of the key executioners of programmed cell death, being responsible for the proteolytic cleavage of several proteins involved in the apoptotic signaling pathway, such as PARP (poly-ADP ribose polymerase).[45] In physiological conditions, caspase-3 exists as a procaspase which is inactive. Activation of the apoptotic cascade leads to the proteolytic processing of the caspase-3 inactive zymogen into activated p17 and p12 subunits. Thus, detection of p17 fragment represents a unique and sensitive indicator of early apoptotic stages. The absence of caspase-3 fragmentation, upon delivery of SWCNT−AAF to macrophages, confirms that CNT preparations are indeed not cytotoxic, allowing us also to exclude SWCNT-induced apoptotic events. In contrast to our findings, Mahmood *et al.* have demonstrated that exposure of osteoblast and cervical cancer cell lines to SWCNTs induces caspase-3 activation.[46] Similarly, significant levels of PARP cleavage were found in mesothelial cells treated with raw SWCNTs.[39] Compared to these studies, where as-produced CNTs have been employed, we used ultrashort CNT fragments which have been functionalized so as to render them more soluble and dispersed than untreated nanotubes. These CNTs, for the reasons explained above, are expected to not produce cytotoxic effects. Since cell death can occur also *via* necrosis and CNTs have been shown to interfere with certain colorimetric assays used to test cytotoxicity, the release of lactate dehydrogenase (LDH) in the culture medium of SWCNT-treated cells was evaluated, as well. Indeed, LDH is a stable cytoplasmic enzyme present in most cells which is promptly released upon loss of membrane integrity. Thus, it is considered an indicator of irreversible cell death due to cell membrane damage.[47] The activity of LDH can be determined by an enzymatic assay which measures the oxidation of NADH to NAD+ at 340 nm.[48] Three independent experiments, using different SWCNT−AAF preparations and cells isolated from different donors, have been performed, and data were expressed as the mean of LDH units (U), released in the culture medium, ± SEM, and no significant differences were observed after overnight incubation of the cells with SWCNT−AAF or the vehicle (0.011 ± 0.004 U *vs* 0.016 ± 0.003 U). As positive control, untreated cells were lysed by adding 0.1% (v/v) Nonidet-P40 detergent directly to the culture medium. In that case, the LDH activity assayed was 0.124 ± 0.010 U, which represents the total LDH amount (intracellular and released). Compared to this value, the released LDH found in CNT- or vehicle-treated cells represented only the 9−13%, which is consistent with the physiological cell death occurring in cell cultures. After 5 days from SWCNT administration, the released LDH was still not significantly different

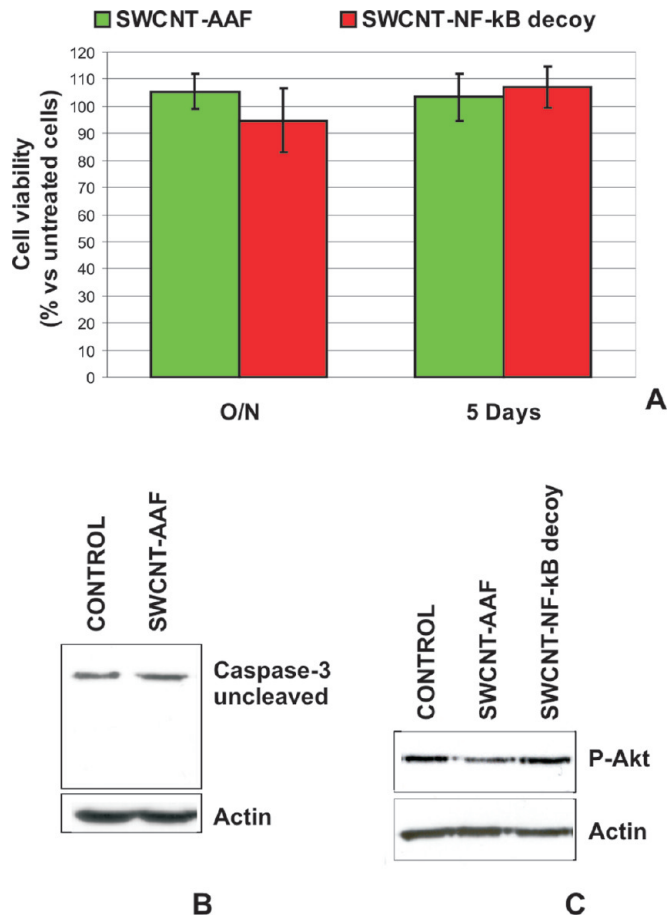

Figure 8. Cytotoxicity of SWCNT. (A) Cells were treated overnight (O/N) with SWCNT−AAF or SWCNT−NF-κB decoy. The day after, the medium was changed and cell viability was measured immediately or after 5 days of culture by MTS assay. All of the values are referred to cells left untreated. The graph shows the results of at least three independent experiments (±SEM). (B) Cells, treated as in A, were harvested after overnight incubation. Cell extracts were submitted to SDS-PAGE and western immunoblotting analysis with an antibody against phospho-Akt (P-Akt) or caspase-3. An actin antibody was used as loading control.

from that found in the culture medium of vehicle-treated cells (0.021 ± 0.018 U *vs* 0.023 ± 0.019 U). Again, these values were the 12−13% of total LDH activity which, at this time point, corresponded to 0.176 ± 0.032 U. On the whole, data deriving from the LDH assay agree with both results of the MTS assay and the inability to observe caspase-3 cleavage, thus further supporting the conclusion that SWCNT-O are not cytotoxic, at least when they are functionalized.

The only difference noted between untreated and SWCNT-treated cells was a slight decrease in Akt phosphorylation in cells receiving SWCNT−AAF but not in those exposed to SWCNT−NF-κB decoys (Figure 8C). It has been reported that Akt is constitutively expressed and activated by phosphorylation in human macrophages.[49] In addition, it has been demonstrated that inhibition of Akt activation results in macrophage apoptosis mediated through the activation of caspase-9 and -3.[49] Although activated Akt is known to be required for macrophage survival, the decreased phosphorylation

observed did not apparently affect cell viability, as assessed by MTS assay (Figure 8A) and LDH release, nor induced caspase-3 cleavage (Figure 8B). Thus, further experiments will be necessary to better understand intracellular pathways eventually affected by exposure to SWCNTs.

CONCLUSIONS

The lack of appropriate vectors for delivering ODN decoy therapeutics still limits their application to the clinic, although these molecules have demonstrated high efficacy and specificity of action as gene expression modulators. It has been recently demonstrated that cellular uptake of CNTs largely depends on their length with short nanotubes able to penetrate the cell membrane more efficiently than longer nanotubes.[50] In agreement with these observations, acid-treated SWCNTs have been shown to more frequently enter the cytoplasm of macrophages than longer untreated SWCNTs. In addition, oxidized CNTs seem noncytotoxic, at least when they are functionalized, thus making them ideal platforms for the delivery of therapeutics.[44] In this context, we have established oxidized ultrashort SWCNTs as a safe and efficient nonviral vector for intracellular delivery of ODN decoy molecules to human macrophages.

Macrophages are the major source of inflammatory mediators that, when chronically expressed, can induce a variety of autoimmune and inflammatory disorders.[51] On the other hand, many genes encoding cytokines, cytokine receptors, cell adhesion molecules, chemoattractant proteins, and growth factors are positively regulated by NF-κB.[6] In this scenario, the delivery efficiency of SWCNT-O and the strong biological effect of NF-κB decoy covalently bound to SWCNT-O suggest a novel strategy to control the inflammatory reaction when becomes aberrant, dysregulated, and cause of disease states.

METHODS

Oligonucleotides. Upper strand (5′-TAAGAGGGAAATTCCGGGAAATTCCTACAT-3′) and reverse-complement phosphodiester oligonucleotides, containing two tandemly repeated copies of the NF-κB binding sequence, found in the PRDII domain of the human interferon-β (IFN-β) promoter, were custom synthesized by Thermo Fisher Scientific GmbH (Ulm, Germany) as HPLC-purified products. The upper strand contained an amino functional group linked to the 5′ end through a six atom carbon spacer. For uptake studies, a FAM-labeled reverse strand was employed. As a control, a double-stranded ODN, where the κB sites have been destroyed by randomizing the corresponding sequences (SCRAMBLED decoy) (5′-TAAGAAACCATGGTGAACCATGGTGTACAT-3′), was used. Oligonucleotides were suspended in 100 mM Hepes/KOH and 1 mM EDTA, pH 7.5, and mixed to obtain stock solutions of double-stranded decoy molecules with a final concentration of 100 μM. Annealing was performed in a thermocycler according to the following temperature profile: 5 min at 100 °C, followed by a temperature reduction to 37 °C over 60 min, and from 37 to 4 °C over 30 min.

SWCNT Oxidation and Cutting. SWCNTs were purchased from Carbon Nanotechnologies Incorporated (Houston, TX) and were oxidized and cut as described essentially by Kam and Dai.[44] Characterization of oxidized SWCNTs was performed by Fourier transform infrared spectroscopy (FTIR), while total acidic sites have been determined by treating a fixed amount of SWCNT-O with an excess of NaOH and back-titrating with HCl, as essentially described by Hu *et al.*[52] The estimated amount of −COOH groups was around 2.36 μmol/mg SWCNTs. Detailed protocols used for SWCNT oxidation and titration are reported under Supporting Information. This section also contains data concerning the characterization of SWCNT-O.

Coupling of ODN Decoys to Oxidized SWCNTs. The primary amine on the 5′ end of the ODN decoy sense strand was coupled to SWCNT *via* carbodiimide activation of the carboxylic acid groups generated in the oxidation of SWCNTs. Briefly, SWCNT-O were suspended in distilled water at a final concentration of 8 mg/mL and tip sonicated for 15 min at 50 W, four times. Sonication was performed with a Labsonic 1510 Sonicator (Braun, Melsungen, Germany) equipped with a 4 mm probe. The suspension was then centrifuged at 12 000 rpm in an Eppendorf centrifuge for 60 min to remove unsuspended bundled CNTs. The supernatant was recovered and centrifuged again for 30 min. SWCNT-O concentration in the supernatant was determined spectrophotometrically at 808 nm using DMSO-dissolved SWCNT-O as a standard ($R^2 = 0.99$). SWCNT-O at a concentration of 0.17 mg/mL (~400 μM COOH) were incubated for 30 min at RT with 40 mM EDAC (Sigma-Aldrich, Steinheim, Germany) and 10 mM NHSS (Invitrogen, Eugene, OR), unless otherwise specified, in 1 mM MES buffer (2-(*N*-morpholino)ethanesulfonic acid), pH 5.5. During this incubation time, the mixture was maintained under constant stirring and tip-sonicated 2 min at 25 W, four times. Ten microliters of activated SWCNT-O was then mixed with 90 μL of amino-modified double-stranded ODN (100 μM), and the pH was adjusted to 8.0 with KOH. A parallel reaction was set with 5-(aminoacetamido)fluorescein (fluoresceinyl glycine amide) (Life Technologies Corporation, Carlsbad, CA) under the same experimental conditions to obtain fluorescein-labeled SWCNTs. Reaction was left to occur for 2 h at 37 °C and continued overnight at +4 °C. To remove unreacted ODN or fluorescein, the solution was repeatedly diluted in PBS buffer and passed through Amicon Ultra-4 centrifugal filter devices (100 kDa cutoff) (Millipore, Billerica, MA) in order to drop the concentration of unreacted molecules below femtomolar. Centrifugation was performed in a GPR centrifuge (Beckman Coulter Inc., Brea, CA) equipped with a swinging bucket rotor. The retentate was recovered, centrifuged at 12 000 rpm in an Eppendorf centrifuge for 30 min a +4 °C, and the supernatant was used in subsequent experiments.

Cell Culture and Treatment. HeLa cells were purchased from the American Type Culture Collection (ATCC, Rockville, MD). Cells were grown in RPMI 1640 medium, supplemented with 10% fetal bovine serum (heat inactivated for 30 min at 56 °C), 2 mM glutamine, 100 μg/mL streptomycin, and 100 U/mL penicillin (all purchased from Cambrex Bioscience, Verviers, Belgium), at 37 °C in a 5% CO_2 atmosphere. Cells were plated at a density of 5×10^5 cells/60 mm diameter culture dish. The day after, cells were stimulated with 1 ng/mL tumor necrosis factor-α (TNF-α) (Boehringer Mannheim Biochemia, Mannheim, Germany) for 1 h at 37 °C. After stimulation, cells were washed and harvested with cold phosphate-buffered saline. Nuclear proteins were obtained by low salt/detergent cell lysis followed by high salt extraction of nuclei as previously described.[53]

Mononuclear cells (MCs) were isolated from pathogen-negative buffy coats obtained from the Transfusional Center of the local hospital (Urbino, Italy) by separation on Lymphoprep (Axis-Shield, Oslo, Norway; specific density 1.077). MCs (8×10^5 cells/well) were seeded onto SuwonLab-Tek II chamber slide system, 8-well glass slide (Nalgene Nunc International, Naperville, IL), and monocytes were separated from lymphocytes by adherence overnight at 37 °C. After removal of nonadhering cells by re-

peated washes, cells were cultured in RPMI 1640 medium as described above. The culture medium was changed every 2 days, and after 7 days of culture, the vast majority of the adherent cells were differentiated macrophages, as revealed by immunostaining with an anti-CD14 antibody (R&D Systems Inc., Minneapolis, MN). On day 8−10 of culture, monocyte-derived macrophages were incubated overnight with SWCNT−ODN conjugates (the NF-kB or the SCRAMBLED decoy) or SWCNT−AAF diluted in incomplete RPMI. When indicated, cells were stimulated with 1 μg/mL lipopolysaccharide (LPS) from *Escherichia coli* 0111:B4 (Sigma-Aldrich).

Electrophoretic Mobility Shift Assay (EMSA). Quantification of conjugated ODN was determined by competitive EMSA. The assay was performed essentially as previously described with some modifications.[53] Briefly, nuclear extracts (0.34 mg/mL) from TNF-α-stimulated HeLa cells were preincubated with 0.2 mg/mL double-stranded nonspecific DNA competitor poly(dI-dC) (Amersham Pharmacia Biotech, Piscataway, NJ) for 10 min on ice in binding buffer (20 mM Hepes/KOH, pH 7.9, 0.1 M KCl, 5% (v/v) glycerol, 0.2 mM EGTA, 0.2 mM EDTA, 1 mM dithiothreitol). Aliquots of the mixture corresponding to 5 μg of nuclear extracts were transferred into separate tubes and incubated with increasing volumes of the individual SWCNT−ODN preparations for 20 min on ice. After this period of time, a fixed amount of the corresponding free ^{32}P-end-labeled ODN was added to each tube and the incubation was continued for an additional 30 min. Reaction mixtures were then submitted to electrophoretic separation on 5% (w/v) native polyacrylamide gels (29:1 cross-linked) in Tris-glycine buffer (25 mM Tris base, 192 mM glycine). NF-κB/[^{32}P]ODN complexes were detected and quantified by exposing the dried gel in a Molecular Imager (Bio-Rad Laboratories, Hercules, CA). The values (mean counts) were expressed as % of the value obtained by incubating nuclear extracts with SWCNT−AAF, considered as 100% of specific radioligand binding. Values were fitted with a sigmoidal dose−response equation to estimate the IC_{50} value. Under our experimental conditions, the IC_{50} corresponds to the volume of the preparation which must be added to the reaction to have equimolar concentrations of the cold SWCNT-bound competitor and of the probe and which results in a 50% displacement of the NF-κB molecules bound to the free ^{32}P-labeled ODN. Thus, on the basis of the probe molar concentration added to the reaction and the calculated IC_{50} value, the amount of ODN conjugated to SWCNTs was determined for each coupling reaction.

Atomic Force Microscope Imaging. Atomic force microscope (AFM) analysis was carried out by dropping ODN-functionalized SWCNTs, diluted in 2 mM $MgCl_2$, onto the surface of freshly cleaved mica (muscovite). The droplet was allowed to stand for 20 s at room temperature, after which the substrate was rinsed with Milli-Q water, dried under N_2, and used for AFM imaging in non-contact mode by a XE-100 AFM (Park System Corp., Suwon, Korea). The scan frequency was typically between 1 and 8 Hz per line.

Electrospray Ionization Mass Spectrometry. ESI-MS experiments were performed on API 150 EX electrospray single-quadrupole mass spectrometer (Perkin-Elmer, Langen, Germany) set in a full scan mode. The samples were analyzed in positive mode by direct syringe infusion at a flow rate of 10 $\mu L \cdot min^{-1}$. Ionization was performed using a needle voltage of 6000 V. Samples were diluted with an aqueous solution containing 90% (v/v) acetonitrile and 0.1% (v/v) formic acid in order to bring SWCNT concentration to 0.3 μg/mL.

Fluorescence Microscopy. After treatment, cells were washed in PBS and fixed with 3.7% (v/v) formaldehyde in PBS for 30 min at room temperature. DNA was stained with 4,6-diamino-2-phenylindole (DAPI) at a final concentration of 0.2 μg/mL. Samples mounted in gelvatol were observed by a Leica (Wetzlar, Germany) DMLB fluorescent microscope equipped with a DC300F CCD camera. Images were processed by NIH ImageJ software (Rasband, W.S., ImageJ, National Institutes of Health, Bethesda, Maryland, http://rsb.info.nih.gov/ij/, 1997−2004).

RNA Isolation and Quantitative Real-Time PCR. Total RNA was isolated using the RNeasy (plus) mini kit (Qiagen Inc. Valencia, CA) and its concentration accurately determined using the Nanodrop ND-1000 System (NanoDrop Technologies, Wilmington, DE). First-strand cDNA was synthesized with the SuperScript First-Strand Synthesis System for RT-PCR (Invitrogen) and oligo-dT primers (0.5 μg/μL) in a final volume of 20 μL, according to the manufacturer's instructions. The synthesized cDNAs were used as templates in SYBR green quantitative real-time PCR (qRT-PCR) assays, performed with the Hot-Rescue RealTime PCR kit (Diatheva s.r.l., Fano, Italy). PCR reactions were set up in a volume of 25 μL containing 1× Hot-Rescue RealTime Master Mix, 0.2 μM of gene specific primers, 0.625 units of Hot-Rescue DNA polymerase, 5 μL (0.6 ng/μL) of the RNase H-treated cDNA stock, and the $MgCl_2$ concentration specified below for the various targets investigated. DNA amplifications were carried out in 96-well reaction plates using ABI PRISM 7700 sequence detection system platform (Applied Biosystems, Foster City, CA). The qRT-PCR primers (obtained from Sigma-Genosys Ltd., Haverhill, UK) were designed using Primer Express version 2.0 and tested to confirm the appropriate product size and optimal concentrations. Primer sequences, as well as the relative $MgCl_2$ concentration used, were Cox-2 forward, 5′-CACCCATGTCAAAACCGAGG-3′, and reverse, 5′-CCGGTGTTGAGCAGTTTTCTC-3′ (3.5 mM $MgCl_2$); IL-8 forward, 5′-ATGACTTCCAAGCTGGCCGT-3′, and reverse, 5′-CAGCCCTCTTCAAAAACTTCTCC-3′ (2.5 mM $MgCl_2$); IL-23 forward, 5′-CGTCTCCTTCTCCGCTTCA-3′, and reverse, 5′-GTGCCTGGGGTGGTAGATTT-3′ (2.5 mM $MgCl_2$); IkBα forward, 5′-CGCACCTCCACTCCATCCT-3′, and reverse, 5′-ACATCCAGCCCCACACTTCAAC-3′ (3.5 mM $MgCl_2$); b2-microglobulin (*B2M*) forward, 5′-GCCTGCCGTGTGAACCAT-3′, and reverse, 5′-CATCTTCAAACCTCCATGATGCT-3′ (3.5 mM $MgCl_2$). Cycle conditions were 95 °C for 10 min followed by 40 cycles of 15 s at 95 °C, 15 s at 60 °C, and 30 s at 72 °C. Amplification plots were analyzed using SDS 1.9.1 software (Applied Biosystems), and relative expression data were calculated with the $2^{-\Delta\Delta CT}$ method.[54] Thus, the relative abundance of the various genes investigated, normalized to the housekeeping *B2M* gene, was expressed as percent amount in cells receiving SWCNT-conjugated NF-κB or scrambled ODN decoys with respect to the reference sample, represented by cells treated with SWCNT−AAF.

Western Immunoblot. Macrophages were directly harvested in 50 mM Tris-HCl, pH 7.8, 0.25 M sucrose, 2% (w/v) sodium dodecyl sulfate (SDS), supplemented with a commercially available cocktail of protease (Roche Diagnostics GmbH, Mannheim, Germany) and phosphatase (1 mM NaF, 1 mM Na_3VO_4) inhibitors. Lysates were boiled for 5 min, then sonicated at 100 W for 20 s. Cell debris was removed by brief centrifugation (10 min at 12 000*g*). Equal volumes of whole-cell extracts were resolved by SDS-PAGE, and gels were electroblotted onto a nitrocellulose membrane (0.2 μm pore size) (BioRad). The blots were probed with the primary antibodies listed below, and bands were detected using horseradish peroxidase conjugated secondary antibody (BioRad). Peroxidase activity was detected with the enhanced chemiluminescence detection method (ECL Kit, Amersham Biosciences, Arlington Heights, IL). The antibodies used in this study were anti-phospho-Akt; anti-caspase-3 (Cell Signaling Technology, Beverly, MA), and anti-actin (Sigma-Aldrich).

Cell Toxicity Assays. Cytotoxicity of SWCNTs was assessed by using a CellTiter-96 aqueous one solution kit from Promega (Madison, WI). This assay is based on the reduction of the MTS reagent [3-(4,5-dimethylthiazol-2yl)-5-(3-carboxymethoxyphenyl)-2-(4-sulfophenyl)2*H*-tetrazolium, inner salt] into a colored formazan product that is soluble in tissue culture medium. This conversion is accomplished by NADPH or NADH produced by dehydrogenase enzymes in metabolically active cells. The quantity of formazan product, as measured by the absorbance at 490 nm, is directly proportional to the number of living cells in culture. It is worth noting that, in contrast to the MTT, the MTS assay does not involve the formation of insoluble formazan crystals, which associate with CNTs, giving false positive results.[55] As a measure of cell membrane damage, LDH activity in the culture medium from SWCNT-treated and control groups (vehicle receiving cells) was spectrophotometrically determined following the oxidation of NADH to NAD+ at 340 nm, as reported by Beutler.[48] LDH catalyzes the reduction of pyruvate to lactate by NADH. One mole of NADH is oxidized for each mole of pyruvate reduced ($\varepsilon = 6.22$ for NADH).

Acknowledgment. This work was supported by the European project no. 5000804-2, NACBO, "Novel and Improved Nanomaterials Chemistries and Apparatus for Nanobiotechnology" granted to M. Magnani.

Supporting Information Available: Detailed preparation and characterization of oxidized SWCNTs. This material is available free of charge *via* the Internet at http://pubs.acs.org.

REFERENCES AND NOTES

1. Patil, S. D.; Rhodes, D. G.; Burgess, D. J. DNA-Based Therapeutics and DNA Delivery Systems: A Comprehensive Review. *AAPS J.* **2005**, *7*, E61–E77.
2. Tomita, N.; Ogihara, T.; Morishita, R. Transcription Factors as Molecular Targets: Molecular Mechanisms of Decoy ODN and Their Design. *Curr. Drug Targets* **2003**, *4*, 603–608.
3. Mann, M. J.; Dzau, V. J. Therapeutic Applications of Transcription Factor Decoy Oligonucleotides. *J. Clin. Invest.* **2000**, *106*, 1071–1075.
4. Igawa, K.; Satoh, T.; Yokozeki, H. A Therapeutic Effect of STAT6 Decoy Oligodeoxynucleotides Ointment in Atopic Dermatitis: A Pilot Study in Adults. *Br. J. Dermatol.* **2009**, *160*, 1124–1126.
5. Sen, M.; Tosca, P. J.; Zwayer, C.; Ryan, M. J.; Johnson, J. D.; Knostman, K. A.; Giclas, P. C.; Peggins, J. O.; Tomaszewski, J. E.; McMurray, T. P.; *et al.* Lack of Toxicity of a STAT3 Decoy Oligonucleotide. *Cancer Chemother. Pharmacol.* **2009**, *63*, 983–995.
6. Baldwin, A. S., Jr. Series Introduction: the Transcription Factor NF-κB and Human Disease. *J. Clin. Invest.* **2001**, *107*, 3–6.
7. Isomura, I.; Morita, A. Regulation of NF-κB Signaling by Decoy Oligodeoxynucleotides. *Microbiol. Immunol.* **2006**, *50*, 559–563.
8. Higuchi, Y.; Kawakami, S.; Nishikawa, M.; Yamashita, F.; Hashida, M. Intracellular Distribution of NFκB Decoy and Its Inhibitory Effect on TNFα Production by LPS Stimulated RAW 264.7 Cells. *J. Controlled Release* **2005**, *107*, 373–382.
9. El-Andaloussi, S.; Johansson, H.; Magnusdottir, A.; Järver, P.; Lundberg, P.; Langel, U. TP10, a Delivery Vector for Decoy Oligonucleotides Targeting the Myc Protein. *J. Controlled Release* **2005**, *110*, 189–201.
10. Gao, H.; Xiao, J.; Sun, Q.; Lin, H.; Bai, Y.; Yang, L.; Yang, B.; Wang, H.; Wang, Z. A Single Decoy Oligodeoxynucleotides Targeting Multiple Oncoproteins Produces Strong Anticancer Effects. *Mol. Pharmacol.* **2006**, *70*, 1621–1629.
11. De Rosa, G.; De Stefano, D.; Laguardia, V.; Arpicco, S.; Simeon, V.; Carnuccio, R.; Fattal, E. Novel Cationic Liposome Formulation for the Delivery of an Oligonucleotide Decoy to NF-κB into Activated Macrophages. Eur. *J. Pharm. Biopharm.* **2008**, *70*, 7–18.
12. Tomita, N.; Morishita, R.; Yamamoto, K.; Higaki, J.; Dzau, V. J.; Ogihara, T.; Kaneda, Y. Targeted Gene Therapy for Rat Glomerulonephritis Using HVJ-Immunoliposomes. *J. Gene Med.* **2002**, *4*, 527–535.
13. Ehsan, A.; Mann, M. J.; Dell'Acqua, G.; Dzau, V. J. Long-Term Stabilization of Vein Graft Wall Architecture and Prolonged Resistance to Experimental Atherosclerosis after E2F Decoy Oligonucleotide Gene Therapy. *J. Thorac. Cardiovasc. Surg.* **2001**, *121*, 714–722.
14. Yang, W.; Thordarson, P.; Gooding, J. J.; Ringer, S. P.; Braet, F. Carbon Nanotubes for Biological and Biomedical Applications. *Nanotechnology* **2007**, stacks.iop.org/Nano/18/412001.
15. Wu, Y.; Philips, J. A.; Liu, H.; Yang, R.; Tan, W. Carbon Nanotubes Protect DNA Strand During Cellular Delivery. *ACS Nano* **2008**, *2*, 2023–2028.
16. Liu, Z.; Winters, M.; Holodniy, M.; Dai, H. siRNA Delivery into Human T Cells and Primary Cells with Carbon-Nanotube Transporters. *Angew. Chem., Int. Ed.* **2001**, *46*, 2023–2027.
17. Kam, N. W.; Liu, Z.; Dai, H. Functionalization of Carbon Nanotubes *via* Cleavable Disulfide Bonds for Efficient Intracellular Delivery of siRNA and Potent Gene Silencing. *J. Am. Chem. Soc.* **2005**, *127*, 12492–12493.
18. Zhang, Z.; Yang, X.; Zhang, Y.; Zeng, B.; Wang, S.; Zhu, T.; Roden, R. B.; Chen, Y.; Yang, R. Delivery of Telomerase Reverse Transcriptase Small Interfering RNA in Complex with Positively Charged Single-Walled Carbon Nanotubes Suppresses Tumor Growth. *Clin. Cancer Res.* **2006**, *12*, 4933–4939.
19. Cui, D.; Tian, F.; Coyer, S. R.; Wang, J.; Pan, B.; Gao, F.; He, R.; Zhang, Y. Effects of Antisense-Myc-Conjugated Single-Walled Carbon Nanotubes on HL-60 Cells. *J. Nanosci. Nanotechnol.* **2007**, *7*, 1639–1646.
20. Crinelli, R.; Bianchi, M.; Gentilini, L.; Magnani, M. Design and Characterization of Decoy Oligonucleotides Containing Locked Nucleic Acids. *Nucleic Acids Res.* **2002**, *30*, 2435–2443.
21. Berkowitz, B.; Huang, D. B.; Chen-Park, F. E.; Sigler, P. B.; Ghosh, G. The X-ray Crystal Structure of the NF-κB p50.p65 Heterodimer Bound to the Interferon β-κB Site. *J. Biol. Chem.* **2002**, *277*, 24694–24700.
22. Zheng, M.; Jagota, A.; Strano, M. S.; Santos, A. P.; Barone, P.; Chou, S. G.; Diner, B. A.; Dresselhaus, M. S.; McLean, R. S.; Onoa, G. B.; *et al.* Structure-Based Carbon Nanotube Sorting by Sequence-Dependent DNA Assembly. *Science* **2003**, *302*, 1545–1548.
23. Gigliotti, B.; Sakizzie, B.; Bethune, D. S.; Shelby, R. M.; Cha, J. N. Sequence-Independent Helical Wrapping of Single-Walled Carbon Nanotubes by Long Genomic DNA. *Nano Lett.* **2006**, *6*, 159–164.
24. Zhao, X.; Johnson, J. K. Simulation of Adsorption of DNA on Carbon Nanotubes. *J. Am. Chem. Soc.* **2007**, *129*, 10438–10445.
25. Singh, R.; Pantarotto, D.; McCarthy, D.; Chaloin, O.; Hoebeke, J.; Partidos, C. D.; Briand, J. P.; Prato, M.; Bianco, A.; Kostarelos, K. Binding and Condensation of Plasmid DNA onto Functionalized Carbon Nanotubes: Toward the Construction of Nanotube-Based Gene Delivery Vectors. *J. Am. Chem. Soc.* **2005**, *127*, 4388–4396.
26. Hazani, M.; Naaman, R.; Hennrich, F.; Kappes, M. M. Confocal Fluorescence Imaging of DNA-Functionalized Carbon Nanotubes. *Nano Lett.* **2003**, *3*, 153–155.
27. Gao, Y.; Kyratzis, I. Covalent Immobilization of Proteins on Carbon Nanotubes Using the Cross-Linker1-Ethyl-3-(3-dimethylaminopropyl)carbodiimide—A Critical Assessment. *Bioconjugate Chem.* **2008**, *19*, 1945–1950.
28. Chen, Z.; Kobashi, K.; Rauwald, U.; Booker, R.; Fan, H.; Hwang, W. F.; Tour, J. M. Soluble Ultra-Short Single-Walled Carbon Nanotubes. *J. Am. Chem. Soc.* **2006**, *128*, 10568–10571.
29. Forrest, A. G.; Alexander, A. J. A Model for the Dependence of Carbon Nanotube Length on Acid Oxidation Time. *J. Phys. Chem. C* **2007**, *111*, 10792–10798.
30. Kim, J. M.; Jung, H. S.; Park, J. W.; Lee, H. Y.; Kawai, T. AFM Phase Lag Mapping for Protein−DNA Oligonucleotide Complexes. *Anal. Chim. Acta* **2004**, *525*, 151–157.
31. Avdoshenko, S. M.; Loffe, I. N.; Kozlov, A. A.; Markov, V. Y.; Nikoolaev, E. N.; Sidorov, L. N. Novel Possibilities in the Study of Isolated Carbon Nanotubes. *Rapid Commun. Mass Spectrom.* **2008**, *22*, 1372–1376.
32. Lukacs, G. L.; Haggie, P.; Seksek, O.; Lechardeur, D.; Freedman, N.; Verkman, A. S. Size-Dependent DNA Mobility in Cytoplasm and Nucleus. *J. Biol. Chem.* **2000**, *275*, 1625–1629.
33. Koki, A.; Khan, N. K.; Woerner, B. M.; Dannenberg, A. J.; Olson, L.; Seibert, K.; Edwards, D.; Hardy, M.; Isakson, P.; Masferrer, J. L. Cyclooxygenase-2 in Human Pathological Disease. *Adv. Exp. Med. Biol.* **2002**, *507*, 177–184.
34. Pease, J. E.; Sabroe, I. The Role of Interleukin-8 and Its Receptors in Inflammatory Lung Disease: Implication for Therapy. *Am J. Respir. Med.* **2002**, *1*, 19–25.
35. Tan, Z. Y.; Bealgery, K. W.; Fang, Y.; Gong, Y. M.; Bao, S. Interleukin-23: Immunological Roles and Clinical Implications. *Int. J. Biochem. Cell Biol.* **2009**, *41*, 733–735.

36. Saccani, S.; Pantano, S.; Natoli, G. Two Waves of Nuclear Factor κB Recruitment To Target Promoters. *J. Exp. Med.* **2001**, *193*, 1351–1359.
37. Nelson, D. E.; Ihekwaba, A. E.; Elliott, M.; Johnson, J. R.; Gibney, C. A.; Foreman, B. E.; Nelson, G.; See, V.; Horton, C. A.; Spiller, D. G.; *et al.* Oscillations in NF-κB Signaling Control the Dynamics of Gene Expression. *Science* **2004**, *306*, 704–708.
38. Firme, C. P.; Bandaru, P. R. Toxicity Issues in the Application of Carbon Nanotubes to Biological Systems. *Nanomedicine* **2010**, *6*, 245–256.
39. Pacurari, M.; Yin, X. J.; Zhao, J.; Ding, M.; Leonard, S. S.; Schwegler-Berry, D.; Ducatman, B. S.; Sbarra, D.; Hoover, M. D.; Castranova, V.; *et al.* Raw Single-Wall Carbon Nanotubes Induce Oxidative Stress and Activate MAPKs, AP-1, NF-κB, and Akt in Normal and Malignant Human Mesothelial Cells. *Environ. Health. Perspect.* **2008**, *116*, 1211–1217.
40. Porter, A. E.; Gass, M.; Muller, K.; Skepper, J. N.; Midgley, P. A.; Welland, M. Direct Imaging of Single-Walled Carbon Nanotubes in Cells. *Nat. Nanotechnol.* **2007**, *11*, 713–717.
41. Kolosnjaj-Tabi, J.; Hartman, K. B.; Boudjemaa, S.; Ananta, J. S.; Morgant, G.; Szwarc, H.; Wilson, L. J.; Moussa, F. *In Vivo* Behavior of Large Doses of Ultrashort and Full-Length Single-Walled Carbon Nanotubes after Oral and Intraperitoneal Administration to Swiss Mice. *ACS Nano* **2010**, *4*, 1481–1492.
42. Porter, A. E.; Gass, M.; Bendall, J. S.; Muller, K.; Goode, A.; Skepper, J. N.; Midgley, P. A.; Welland, M. Uptake of Noncytotoxic Acid-Treated Single-Walled Carbon Nanotubes into the Cytoplasm of Human Macrophage Cells. *ACS Nano* **2009**, *3*, 1485–1492.
43. Saxena, R. K.; Williams, W.; McGee, J. K.; Daniels, M. J.; Boykin, E.; Gilmour, M. I. Enhanced *In Vitro* and *In Vivo* Toxicity of Poly-Dispersed Acid-Functionalized Single-Wall Carbon Nanotubes. *Nanotoxicology* **2007**, *1*, 291–300.
44. Kam, N. W.; Dai, H. Carbon Nanotubes as Intracellular Protein Transporters: Generality and Biological Functionality. *J. Am. Chem. Soc.* **2005**, *127*, 6021–6026.
45. Nicholson, D. W.; Ali, A.; Thornberry, N. A.; Vaillancourt, J. P.; Ding, C. K.; Gallant, M.; Gareau, Y.; Griffin, P. R.; Labelle, M.; Lazebnik, Y. A.; *et al.* Identification and Inhibition of the ICE/CED-3 Protease Necessary for Mammalian Apoptosis. *Nature* **1995**, *376*, 37–43.
46. Mahmood, M.; Casciano, D. A.; Mocan, T.; Iancu, C.; Xu, Y.; Mocan, L.; Iancu, D. T.; Dervishi, E.; Li, Z.; Abdalmuhsen, M.; *et al.* Cytotoxicity and Biological Effects of Functional Nanomaterials Delivered to Various Cell Lines. *J. Appl. Toxicol.* **2010**, *30*, 74–83.
47. Walker, V. G.; Li, Z.; Hulderman, T.; Schwegler-Berry, D.; Kashon, M. L.; Simeonova, P. P. Potential *In Vitro* Effects of Carbon Nanotubes on Human Aortic Endothelial Cells. *Toxicol. Appl. Pharmacol.* **2009**, *236*, 319–328.
48. Beutler, E. Lactate Deydrogenase (LDH). In *Red Cell Metabolism. A Manual of Biochemical Methods*; Beutler, E., Ed.; Grune and Stratton, Inc.: New York, 1984; pp 65−66.
49. Liu, H.; Perlman, H.; Pagliari, L. J.; Pope, R. M. Constitutively Activated Akt-1 Is Vital for the Survival of Human Monocyte-Differentiated Macrophages: Role of Mcl-1, Independent of Nuclear Factor (NF)-κB, Bad, or Caspase Activation. *J. Exp. Med.* **2001**, *194*, 113–125.
50. Raffa, V.; Ciofani, G.; Nitodas, S.; Karachalios, T.; D'Alessandro, D.; Masini, M.; Cuscheri, A. Can the Properties of Carbon Nanotubes Influence Their Internalization by Living Cells? *Carbon* **2008**, *46*, 1600–1610.
51. Ma, Y.; Pope, R. M. The Role of Macrophages in Rheumatoid Arthritis. *Curr. Pharm. Des.* **2005**, *11*, 569–580.
52. Hu, H.; Bhowmik, P.; Zhao, B.; Hamon, M. A.; Itkis, M. E.; Haddon, R. C. Determination of the Acidic Sites of Purified Single-Walled Carbon Nanotubes by Acidic-Base Titration. *Chem. Phys. Lett.* **2001**, *345*, 25–28.
53. Crinelli, R.; Bianchi, M.; Gentilini, L.; Palma, L.; Sørensen, M. D.; Bryld, T.; Babu, R. B.; Arar, K.; Wengel, J.; Magnani, M. Transcription Factor Decoy Oligonucleotides Modified with Locked Nucleic Acids: An *In Vitro* Study To Reconcile Biostability with Binding Affinity. *Nucleic Acids Res.* **2004**, *32*, 1874–1885.
54. Livak, K. J.; Schmittgen, T. D. Analysis of Relative Gene Expression Data Using Real-Time Quantitative PCR and the $2^{-\Delta\Delta CT}$ Method. *Methods* **2001**, *25*, 402–408.
55. Wörle-Knirsch, J. M.; Pulskamp, K.; Krug, H. F. Oops They Did it Again! Carbon Nanotubes Hoax Scientists in Viability Assays. *Nano Lett.* **2006**, *6*, 1261–1268.